

Heat capacity and thermodynamic properties of crystalline ornidazole (C₇H₁₀ClN₃O₃)

Mei-Han Wang^a, Zhi-Cheng Tan^{a,*}, Xiao-Hong Sun^b, Fen Xu^a,
Yuan-Fa Liu^b, Li-Xian Sun^a, Tao Zhang^a

^a Thermochemistry Laboratory, Dalian Institute of Chemical Physics, Chinese Academy of Sciences,
457 Zhoushan Road, Dalian 116023, China

^b College of Chemical Engineering, Northwest University, Xi'an 710069, China

Received 5 September 2003; received in revised form 5 November 2003; accepted 11 November 2003

Abstract

The molar heat capacities of 1-(2-hydroxy-3-chloropropyl)-2-methyl-5-nitroimidazole (Ornidazole) (C₇H₁₀ClN₃O₃) with purity of 99.72 mol% were measured with an adiabatic calorimeter in the temperature range between 79 and 380 K. The melting-point temperature, molar enthalpy, $\Delta_{\text{fus}}H_{\text{m}}$, and entropy, $\Delta_{\text{fus}}S_{\text{m}}$, of fusion of this compound were determined to be 358.59 ± 0.04 K, 21.38 ± 0.02 kJ mol⁻¹ and 59.61 ± 0.05 J K⁻¹ mol⁻¹, respectively, from fractional melting experiments. The thermodynamic function data relative to the reference temperature (298.15 K) were calculated based on the heat capacities measurements in the temperature range from 80 to 380 K. The thermal stability of the compound was further investigated by DSC and TG. From the DSC curve an intensive exothermic peak assigned to the thermal decomposition of the compound was observed in the range of 445–590 K with the peak temperature of 505 K. Subsequently, a slow exothermic effect appears when the temperature is higher than 590 K, which is probably due to the further decomposition of the compound. The TG curve indicates the mass loss of the sample starts at about 440 K, which corresponds to the decomposition of the sample.

© 2003 Elsevier B.V. All rights reserved.

Keywords: Ornidazole; Heat capacity; Thermodynamic functions; Adiabatic calorimetry; TG; DSC

1. Introduction

Nitroheterocyclic chemicals have a wide variety of applications, ranging from food preservatives to antibiotics. 5-Nitroimidazoles are a well-established group of antiprotozoan and antibacterial agents. Due to its antimicrobial activity it inhibits the growth of both anaerobic bacteria and certain anaerobic protozoa such as *Trichomonas vaginalis*, *Entamoeba histolytica* and *Giardia lamblia*. 1-(2-Hydroxy-3-chloropropyl)-2-methyl-5-nitroimidazole (Ornidazole) is a member of the nitroimidazole group so it is used for the treatment of susceptible protozoal infections and prophylaxis of anaerobic bacterial infections. It is more effective than metronidazole and tinidazole against amoe-

biasis and equally as effective as metronidazole in relation to trichomoniasis [1].

Ornidazole has a heterocyclic structure consisting of a nitroimidazole-based nucleus with a 2-hydroxy-3-chloropropyl group, in position 1 and a methyl group in position 2. It is synthesized from 5-nitroimidazole derivatives. In order to improve the process of chemical synthesis and increase understanding of the properties of the compound, the thermodynamic properties are needed urgently. However, most previous investigation focuses on researching its pharmaceutical evaluation, the thermodynamic properties of this compound have not been studied so far as we know.

In the present study, the low-temperature heat capacities have been measured in the temperature range from 79 to 380 K with a small sample automated adiabatic calorimeter. The melting temperature, the molar enthalpy and entropy of fusion of the compound were determined. In addition, the further thermal behavior of the compound was investigated

* Corresponding author. Tel.: +86-411-4379215;
fax: +86-411-4691570.

E-mail address: tzc@dicp.ac.cn (Z.-C. Tan).

by differential scanning calorimetry (DSC) and thermogravimetry (TG).

2. Experimental

2.1. Sample preparation

Ornidazole is light yellow crystal. The sample used for the present calorimetric study was prepared according to the procedures given in Neth. patent [2], in which 1-(2,3-epoxypropyl)-2-methyl-5-nitroimidazole was hydrochlorinated with concentrated hydrochloric acid to yield the product. The process is



The crude product was condensed in vacuum and recrystallized from acetone three times. The structure of the product was determined by IR, ^1H NMR and ^{13}C NMR. Its melting point was determined to be 358–360 K with the microscopic melting-point device (Model: BY-1, Yazawa Co., Japan) and its purity was determined to be higher than 99 mol% by HPLC (model: LC-10AT, Shimadzu, Japan) analysis.

2.2. Adiabatic calorimetry

Heat-capacity measurements were carried out with an adiabatic calorimeter. The construction, principle, and calibra-

tion of the calorimetric apparatus were described in detail in literature [3]. The mass of sample loaded in a calorimeter cell was 1.6647 g, which is equivalent to 7.580 mmol based on its molar mass of 219.63 g mol $^{-1}$.

Prior to the heat-capacity measurements of the sample, the reliability of the calorimetric apparatus was verified by heat-capacity measurements of the reference standard material $\alpha\text{-Al}_2\text{O}_3$. The deviations of our calibration results from the recommended values reported by Xue et al. [4] of the former National Bureau of Standards are within of $\pm 0.2\%$ in the temperature range from 80 to 400 K.

2.3. Thermal analysis

Thermogravimetric (TG) and differential scanning calorimetric studies have been performed by means of a simultaneous TG–DSC 16/18 system (Setaram, France). For thermal decomposition investigations of the compound, open aluminum crucibles, sample weights of 7.8 mg, a linear heating rate of 10 K min $^{-1}$ and flowing nitrogen with 50 ml min $^{-1}$ as purge gas were applied for the measurement.

3. Results and discussion

3.1. Heat capacity

Heat-capacity measurements are listed in Table 1 and plotted in Fig. 1. It can be seen from Fig. 1 that the heat capacities of the sample increase with temperature in a smooth and continuous manner without any thermal anomaly in the range from 79 to 350 K, which means the compound is stable

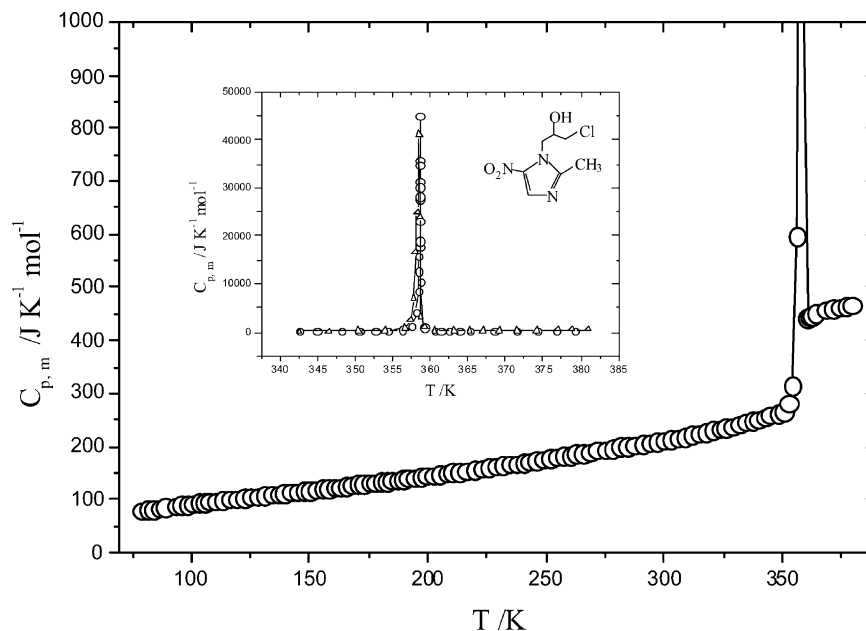


Fig. 1. Experimental molar heat capacity $C_{p,m}$ of ornidazole as a function of temperature (T): Symbol (O) represents the first series of heat-capacity measurements and (Δ) the second series of heat-capacity measurements.

Table 1
The experimental molar heat capacity of ormidazole ($M = 219.63 \text{ g mol}^{-1}$)

T (K)	$C_{p,m}$ (JK^{-1} mol^{-1})	T (K)	$C_{p,m}$ (JK^{-1} mol^{-1})	T (K)	$C_{p,m}$ (JK^{-1} mol^{-1})
Series 1					
78.910	78.56	194.400	141.4	323.343	232.9
81.523	80.56	197.123	142.7	326.167	235.8
84.055	82.17	199.823	144.9	328.968	238.0
86.517	84.18	202.532	146.2	331.745	241.8
88.919	85.84	205.182	148.6	334.498	245.3
93.517	88.29	207.832	149.3	337.133	249.2
95.783	89.70	210.439	151.2	339.907	251.5
98.157	90.97	213.309	152.8	342.578	256.2
100.667	92.53	216.449	155.1	344.928	259.1
103.133	94.04	219.550	157.0	348.232	263.0
105.557	95.46	222.614	159.2	350.466	266.8
107.945	96.55	225.651	161.0	352.631	280.8
110.298	97.68	228.652	162.7	354.385	314.0
113.021	99.12	231.619	164.9	356.317	596.5
116.134	100.8	234.578	166.3	357.573	1374
119.190	102.2	237.518	168.2	358.133	4178
122.198	103.5	240.421	170.2	358.336	8433
125.158	105.5	243.271	172.7	358.435	12702
128.076	106.5	246.119	174.9	358.495	15794
130.956	108.1	248.970	176.3	358.539	17803
133.794	110.0	251.787	178.1	358.576	18963
136.599	111.1	254.578	180.1	358.595	27720
139.365	112.5	257.339	182.8	358.596	44914
142.103	113.6	260.083	184.1	358.596	35897
144.807	114.5	262.803	186.3	358.597	34656
147.507	115.9	265.499	187.9	358.597	31268
150.097	117.9	268.484	190.1	358.598	30119
152.742	119.2	271.763	192.6	358.599	28301
155.342	120.6	275.006	194.3	358.611	23020
157.920	121.8	278.225	196.3	358.663	10488
160.476	123.0	281.415	199.5	359.193	1034
163.007	124.5	284.581	201.2	360.515	442.7
165.517	126.0	287.713	203.1	361.349	444.9
168.006	127.2	290.809	205.7	362.371	448.0
170.475	128.7	293.870	207.3	363.817	451.6
172.925	129.8	296.915	209.6	365.147	453.6
175.356	131.1	299.948	212.1	368.474	456.7
177.769	132.6	302.956	214.2	371.523	459.2
180.163	134.0	305.940	216.1	374.256	462.0
182.542	135.0	308.899	218.9	376.814	464.4
184.903	136.2	311.832	221.3	379.211	467.1
187.248	137.5	314.741	224.6		
189.577	138.9	317.628	227.5		
Series 2					
288.909	205.7	342.589	260.8	359.249	1084
293.593	209.3	346.598	267.3	360.621	437.6
298.267	213.8	350.436	390.6	363.112	442.8
302.910	217.1	354.001	401.8	365.263	446.2
307.516	222.0	356.612	846.9	366.971	449.4
312.087	225.6	357.345	2544	369.130	453.8
316.622	229.6	357.821	7132	371.593	457.5
321.111	234.4	358.082	16516	374.214	460.6
325.545	241.0	358.266	24965	376.984	463.2
329.908	245.4	358.539	41204	378.851	465.9
334.217	252.7	358.627	23790	381.001	468.0
338.453	256.7	358.731	3277		

in this range. However, a thermal anomaly was observed in the temperature range between 350 and 360 K. The thermal anomaly can be ascribed to a solid–liquid phase transition according to the previous melting-point measurement.

The experimental molar heat capacities were fitted to the following polynomial equations in reduced temperature (X) by least square method.

For the solid phase over the temperature range of 79–350 K:

$$C_{p,m} (\text{JK}^{-1} \text{mol}^{-1}) = 154.11 + 85.145X + 11.955X^2 - 13.319X^3 + 5.805X^4 + 21.653X^5$$

where $X = (T - 214.5)/135.5$, and T is the absolute temperature. The correlation coefficient of the fitted curve, $R^2 = 0.9999$. The deviations of experimental results from the smoothed curve lie within $\pm 0.5\%$.

For the liquid phase over the temperature range of 361–379 K:

$$C_{p,m} (\text{JK}^{-1} \text{mol}^{-1}) = 457.919 + 7.276X + 0.020X^2 + 5.056X^3 - 3.171X^4$$

where $X = (T - 370)/9$, $R^2 = 0.9995$. The deviations of experimental results from the smoothed curve lie within $\pm 0.25\%$.

3.2. Melting-point, enthalpy and entropy of fusion

Two series of heat-capacity experiments in the melting region of the compound were carried out using different heating rate in order to verify the repeatability of the melting process. The temperature increment in series 1 was controlled to be about 1–3 K and that of the series 2 was about 3–5 K for each experimental heat-capacity point. The results obtained from the two series of measurement are given in Table 1 and plotted in Fig. 1.

The melting point was determined to be 358.59 ± 0.04 K from the fraction melting experiments in the heat-capacity measurements. The molar enthalpy, $\Delta_{\text{fus}}H_m$, and entropy, $\Delta_{\text{fus}}S_m$, of fusion were derived from the following equations [4].

$$\Delta H_m = \frac{Q - n \int_{T_i}^{T_m} C_{p,s} dT - n \int_{T_m}^{T_f} C_{p,l} dT - n \int_{T_i}^{T_f} H_0 dT}{n} \quad (1)$$

$$\Delta S_m = \frac{\Delta H_m}{T} \quad (2)$$

where T_i is a temperature slightly lower than the initial melting temperature, T_f a temperature slightly higher than the final melting temperature, Q the total energy introduced into the sample cell from T_i to T_f , H_0 the heat capacity of the sample cell from T_i to T_f , $C_{p,s}$ the heat capacity of the sample in solid phase from T_i to T_m , $C_{p,l}$ the heat capacity of the sample in liquid phase from T_m to T_f and n

Table 2

The melting point, enthalpy and entropy of fusion of the sample obtained from two series of heat-capacity measurements

Thermodynamic properties	Series 1 (x_1)	Series 2 (x_2)	Mean value (\bar{x})
Melting point (K)	358.63	358.55	358.59 ± 0.04
$\Delta_{\text{fus}}H_{\text{m}}$ (kJ mol ⁻¹)	21.36	21.39	21.38 ± 0.02
$\Delta_{\text{fus}}S_{\text{m}}$ (J K ⁻¹ mol ⁻¹)	59.56	59.66	59.61 ± 0.05

Table 3

The observed equilibrium temperature (T) and fraction melted (F) during the melting process

$F = q/Q$	$1/F$	T (K)
Series 1		
0.0306	32.65	354.385
0.1106	9.039	357.573
0.2274	4.398	358.133
0.3074	3.253	358.336
0.4070	2.457	358.435
0.4923	2.031	358.495
0.5787	1.728	358.539
0.6299	1.588	358.576
0.7135	1.402	358.595
Series 2		
0.0313	31.98	354.001
0.0659	15.16	356.612
0.1435	6.967	357.721
0.2211	4.523	357.982
0.2560	3.906	358.066

is molar amount of the sample. The results of molar enthalpy and entropy of fusion obtained from the two series of heat-capacity measurements in the range of fusion are listed in Table 2.

3.3. Purity determination

Adiabatic calorimetry provides an accurate way for determining the purity of a substance. The purity of sample can be evaluated from the observed melting-point curve [5,6]. If the liquid solution formed in the premelting region are ideal, and thus obey Raoult's law, the following expression can be used to calculate the purity of the sample:

$$X_2 = \frac{\Delta H_{\text{m}}(T_0 - T_1)}{RT_0^2}; \quad F = \frac{q}{Q}; \quad T_0 - T = \frac{T_0 - T_1}{F}$$

Table 4

The melting temperature and the impurity content obtained from the fraction melting experiment in the range of fusion

	Series 1 (x_1)	Series 2 (x_2)	Mean value (\bar{x})
T_0 (K)	358.77	358.69	358.73 ± 0.04
T_1 (K)	358.63	358.55	358.59 ± 0.04
X_2 (mol%)	0.27	0.29	0.28 ± 0.01

Table 5

Calculated thermodynamic function data of ornidazole

T (K)	$C_{p,m}$ (J K ⁻¹ mol ⁻¹)	$H_T - H_{298.15}$ (kJ mol ⁻¹)	$S_T - S_{298.15}$ (J K ⁻¹ mol ⁻¹)
Crystal			
80	79.17	-30.89	-168.1
85	82.86	-30.48	-163.2
90	86.26	-30.06	-158.4
95	89.41	-29.62	-153.6
100	92.37	-29.16	-149.0
105	95.15	-28.70	-144.5
110	97.81	-28.21	-140.0
115	100.4	-27.72	-135.6
120	102.9	-27.21	-131.3
125	105.3	-26.69	-127.1
130	107.7	-26.16	-122.9
135	110.1	-25.61	-118.8
140	112.6	-25.05	-114.8
145	115.0	-24.49	-110.8
150	117.5	-23.91	-106.9
155	120.0	-23.31	-103.0
160	122.6	-22.71	-99.12
165	125.2	-22.08	-95.32
170	127.9	-21.45	-91.55
175	130.6	-20.81	-87.81
180	133.4	-20.15	-84.11
185	136.3	-19.47	-80.43
190	139.2	-18.78	-76.78
195	142.1	-18.08	-73.14
200	145.2	-17.36	-69.52
205	148.2	-16.63	-65.92
210	151.3	-15.88	-62.33
215	154.4	-15.12	-58.75
220	157.6	-14.33	-55.18
225	160.8	-13.54	-51.62
230	164.0	-12.73	-48.07
235	167.2	-11.90	-44.52
240	170.5	-11.06	-40.98
245	173.8	-10.20	-37.45
250	177.1	-9.318	-33.91
255	180.4	-8.424	-30.38
260	183.7	-7.514	-26.86
265	187.1	-6.587	-23.33
270	190.5	-5.643	-19.81
275	193.9	-4.682	-16.29
280	197.5	-3.704	-12.77
285	201.0	-2.707	-9.255
290	204.7	-1.693	-5.737
295	208.4	-0.6604	-2.218
298.15	210.9	0.0000	0.000
300	212.3	0.3915	1.304
305	216.4	1.463	4.831
310	220.6	2.556	8.366
315	225.0	3.669	11.91
320	229.7	4.806	15.47
325	234.7	5.967	19.05
330	239.9	7.153	22.66
335	245.6	8.367	26.30
340	251.7	9.610	29.98
345	258.2	10.88	33.71
350	265.4	12.19	37.50
Liquid			
360	438.1	33.57	97.11
365	452.7	35.80	103.3
370	457.9	38.08	109.5
375	462.5	40.38	115.7
380	468.1	42.71	121.8

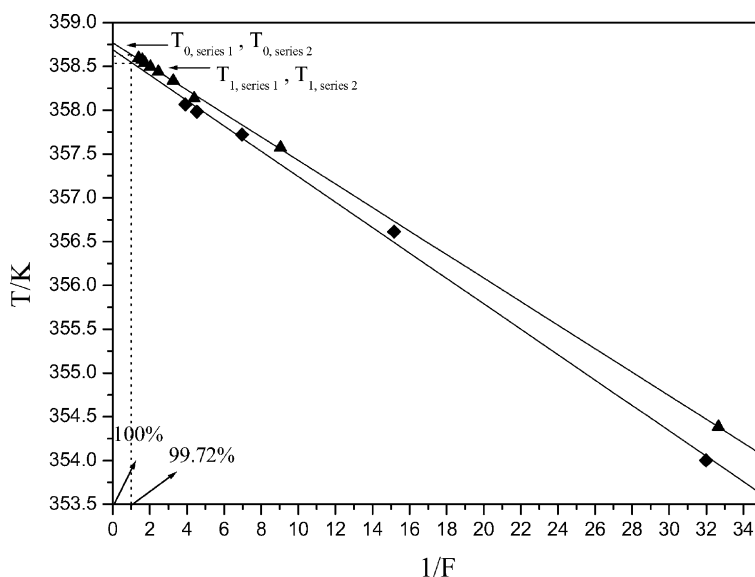


Fig. 2. A plot of temperature vs. reciprocal of fraction melted during the melting process of ornidazole. Symbol (\blacktriangle) represents the first series of fractional melting measurements and (\blacklozenge) the second series of fractional melting measurements.

where F is the fraction of sample melted, ΔH_m the molar enthalpy of fusion, T_0 the triple-point temperature of the pure substance, T_1 the triple-point temperature of the given sample, X_2 is the mole fraction of impurity in liquid solution. The fraction melting data obtained from the heat-capacity measurement in range of fusion are listed in Table 3. The plots of T against $1/F$ in the melting process are shown in Fig. 2. The T_0 is the temperature when $1/F$ equals 0 and T_1 is equivalent to the temperature when $1/F$ is 1. From Fig. 2, the T_0 and T_1 are found to be 358.59 ± 0.04 K and 358.73 ± 0.04 K, respectively. Thus, $X_2 = 0.28 \pm 0.01$ mol% can be calculated, and the purity of ornidazole sample used in the calorimetric experiment accounts to $1 - X_2 = 99.72 \pm 0.01$ mol% (see Table 4).

3.4. Thermodynamic functions of ornidazole

According to the polynomial equation of heat capacity and thermodynamic relationship, the thermodynamic function data of the compound relative to the reference temperature 298.15 K were calculated in the temperature range 80–380 K with an interval of 5 K. The thermodynamic relationships were listed as follows:

$$H_T - H_{298.15} = \int_{298.15}^T C_{p,m} dT \quad (3)$$

$$S_T - S_{298.15} = \int_{298.15}^T \frac{C_{p,m}}{T} dT \quad (4)$$

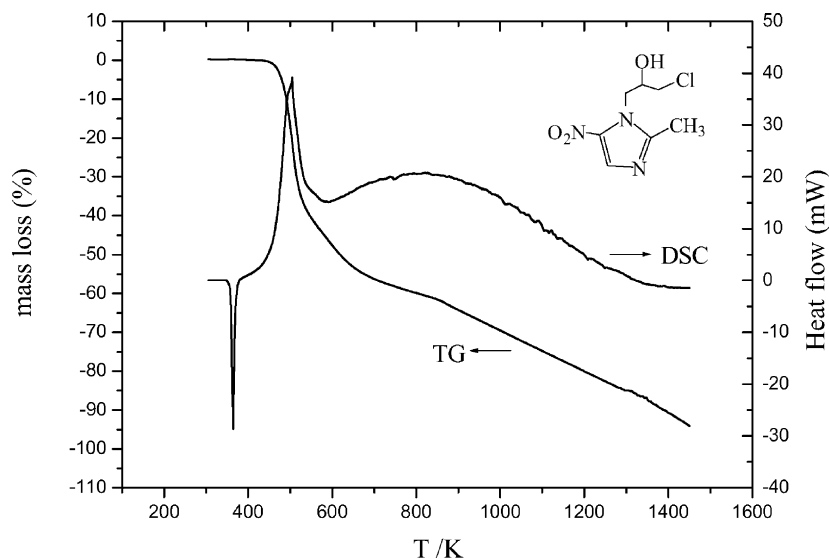


Fig. 3. TG–DSC curves of ornidazole under high purity nitrogen.

The values of thermodynamic function $H_T - H_{298.15}$, $S_T - S_{298.15}$ were listed in Table 5.

3.5. The results of TG–DSC analysis

From the DSC curve in Fig. 3 a sharply endothermic peak assigned to melting process was observed, with the peak temperature of 364 K. Based on the DSC curve the melting point of the sample was determined to be 359 K, which is consistent with the value (358.57 K) obtained from the adiabatic calorimetric measurements. In the range of 445–590 K a sharply exothermic peak was observed with the peak temperature of 505 K, which is ascribed to the thermal decomposition of the compound. When the temperature is higher than 590 K, a slow exothermic effect occurs in the temperature range from 590 to 1450 K, which may be caused by further decomposition of the compound.

From the TG curve, it can be seen that the mass loss of the sample starts at about 440 K. The total mass lost in the heating process from ambient temperature to 1450 K corresponds to 94% of the initial sample weight, remaining 6% (mass) black residual in the crucible. Due to the high purity (99.73 mol%) of the sample, the residual may be the thermal decomposition product of the compound instead of

the heavy impurity contained in the original sample. This case indicates the mass loss of the sample is caused mainly by the decomposition of the sample.

Acknowledgements

The authors gratefully acknowledge the National Natural Science Foundation of China for financial support to this work under the NSFC Grant No. 20073047.

References

- [1] M.M. López Nigro, A.M. Palermo, M.D. Mudry, M.A. Carballo, *Toxicol. In Vitro* 17 (2003) 35–40.
- [2] F. Hoffmann-La Roche & Co., A.-G. *Neth. Appl.* 6,606,853 (1966).
- [3] Z.C. Tan, G.Y. Sun, Y.J. Song, L. Wang, *Thermochim. Acta* 352–353 (2000) 247–253.
- [4] B. Xue, Z.C. Tan, S.W. Lu, S.H. Meng, X.H. Yuan, *Acta Chimica Sinica* 57 (1999) 881–886.
- [5] J.P. McCullough, G. Waddington, *Anal. Chimica Acta* 17 (1957) 80–96.
- [6] J.H. Baley, *J. Phys. Chem.* 63 (1959) 1991–1996.